Journal of Applied Polymer Science

Development of hierarchical structured carbon nanotube-nylon nanofiber mats

Baicheng Weng, Fenghua Xu, Karen Lozano
Department of Mechanical Engineering, University of Texas-Pan American, Edinburg Texas 78539
Correspondence to: K. Lozano (E-mail: lozanok@utpa.edu)

ABSTRACT: A hierarchical nanofiber (NF) structure featuring carbon nanotubes (CNTs) densely attached on the surface of NFs is presented. Nonwoven NF mats made of Nylon 6 (Nylon) were mass produced using the forcespinning® (FS) technology, followed by depositing functionalized CNTs (*f*-CNTs) on the surface of NFs. Strong interfacial adhesion between CNTs and Nylon NFs was developed by the formation of covalent bonds. The morphology, structure, conductivity, and mechanical properties of the developed CNT-Nylon NFs were analyzed. The hierarchical NFs have a 338% improvement in tensile strength without compromising its strain at break. The shielding effectiveness (*SE*) of electromagnetic interference (EMI) was recorded to be 30 dB. These promising characteristics endow novel flexible hierarchical NF mats for applications as EMI shielding materials or smart textiles to mention some. © 2015 Wiley Periodicals, Inc. J. Appl. Polym. Sci. **2015**, *132*, 42535.

KEYWORDS: fibers; graphene and fullerenes; manufacturing; nanotubes

Received 4 February 2015; accepted 25 May 2015
DOI: 10.1002/app.42535

INTRODUCTION

The manufacturing of structured yet compact polymeric fine fibers with diameters ranging from single digit micrometers down to nanometers has been considered of primary importance towards meeting the needs in a variety of fields, such as: filtration, biomedical (tissue engineering, drug-release systems), catalysis, microelectronics, smart textiles, and heating fabrics. The enhanced surface to volume ratio, improved wetting behavior, tailored structural surface, and increased electrical and mechanical properties provide distinct and promising features for a variety of applications where flexible and ultra-lightweight yet strong structures are needed.[1–7]

Several methods exist for the production of fine fibers, such as electrospinning,[4,5] dry-spinning,[8] wet-spinning,[9] and dry-jet wet spinning.[10] Among these, electrospinning has been considered the one with industrial potential; more than 50% of the published articles on NF production have used electrospinning processes. Recently, the development of forcespinning® (FS) technology has gained momentum as a promising method to develop large scale production of nanofibers (NFs) from a variety of materials. FS utilizes centrifugal force to extrude polymer solutions or melts to create fine fibers in the absence of electric fields.[11–18] Fiber jets are formed by high rotational speeds (0−20,000 rpm) of a spinneret using a nozzle. When the centrifugal force and associated hydrostatic pressure exceeds capillary forces that tend to restrict the flow of fluid in the orifice, a jet of polymer solution is ejected. Reduction of fiber diameter occurs by the inertial drag between the fiber and the atmosphere as the polymer solution jet dries. The production rate of lab scale FS equipment is over 1 g min^{-1} per nozzle, which is extremely higher than lab scale electrospinning (0.3 g h^{-1}). Several materials have been successfully spun into fibers, such as poly(vinyl alcohol),[12] pullulan,[13] polyacrylonitrile,[14] poly(methyl methacrylate),[15] polyvinyl butyral,[16] polycaprolactone,[17] and indium-tin oxide[18] to mention some.

Recently, several efforts have been made to prepare carbon nanotube (CNT) reinforced polymeric nanofibers (NFs) to synergistically combine the flexibility and lightweight of nonwoven nanofiber (NF) mats with the enhanced electrical conductivity and mechanical strength observed in CNT/polymer bulk composites.[14–16,19–21] However, this has been hindered by two main issues, the inherent reduction in strain at break just as observed in CNT reinforced polymeric bulk composites and the intrinsic difficulties to obtain an optimum dispersion and distribution of CNT in the solution which inherently presents a challenge to upscale the manufacturing process. The attachment of CNTs on the surface of polymeric NFs by surface absorption, such as it is used in the fabrication of transparent conductive films and electrochemical sensors, has been researched as an alternative method to fabricate flexible, lightweight, and strong nanofiber (NF) structures.[3–7] For instance, Kang *et al.* reported gluing CNTs on the surface of silk resulting in a conductivity

decreasing from 4.4×10^{-15} to 2.4×10^{-4} S cm^{-1}. In our study, CNTs were densely attached through a covalent adsorption method on the surface of Nylon 6 (Nylon) NFs forming a hierarchical structure that combines the versatility, low price, excellent mechanical properties, as well as elasticity and luster of Nylon with the high electrical conductivity and strength of CNTs. The morphology, structure, thermo-physical, and mechanical and electrical properties of the developed hierarchical CNTs/Nylon NFs were characterized.

EXPERIMENTAL

Materials

Nylon 6 ($M_w = 11{,}202$), formic acid (98%, HPLC grade), sulfuric acid (H_2SO_4, 98%), 2,2,2-trifluoroethanol (TFE) anhydrous potassium bromide (KBr, >99%), and nitric acid (HNO_3, 70%) were purchased from Sigma Aldrich. Multi-walled carbon nanotubes (CNTs) (outer diameter 30 nm) were purchased from Cheap Tubes. Deionized water 18 M Ω cm produced from Mill-Q (Millipore Ltd, UK), was used to prepare all of the aqueous solutions. For the spinning of the fibers, a lab scale Cyclone^{TM} L-1000M from Fiberio Technology Corp. was utilized.

Methods

For the production of the Nylon NF mat, a 25 wt % Nylon solution was prepared by dissolving Nylon 6 (Nylon) in formic acid. The solution was fed into the spinneret and spun at a rotational speed of 7000 rpm. Schematics and description of the fiber formation process have been published elsewhere.[11–18] Figure 1 shows a photograph of the developed Nylon nonwoven fiber mat. Samples used here were cut from this mat.

CNTs were functionalized according to Lozano *et al.*[22] Briefly, 500 mg of pristine CNTs were added into a 150 mL mixture of acids (concentrated sulfuric acid (H_2SO_4) and nitric acid (HNO_3) with a volume ratio of 3 : 1), and sonicated for 4 h at 50°C, followed by refluxing the mixture for 12 h at 70°C. The slurry was then diluted with deionized water, and subsequently filtered until a pH of 7 was reached. The CNTs were then dried at 120°C for 24 h. The 0.1 wt % and 0.5 wt % of CNTs aqueous suspensions were prepared by dispersing the functionalized CNTs (*f*-CNTs) through ultrasonic methods. Subsequently, 5 wt % of TFE was added into the suspension to promote attachment of CNTs onto the Nylon NFs. The nonwoven Nylon NF mats were dipped in the CNTs suspension, and then pulled out at a speed of 5 cm min^{-1}, followed by rinsing it with deionized water, and then dried at 140°C for 2 h.

Characterizations

The morphology of the nanofiber (NF) mats was evaluated using a scanning electron microscope (SEM, Sigma VP, Carl Zeiss, Germany). The average fiber diameter and other data related to fiber dimensions were determined by randomly measuring 300 NFs per sample. The measurement was conducted from the SEM images utilizing an image analysis software (JMicroVision V.1.2.7, University of Geneva, Geneva, Switzerland). Thermogravimetric analysis (TGA) was conducted using a TGA-Q500, TA Instruments. Samples of 10 mg were heated on platinum pans from room temperature to 750°C at a heating rate of 10°C min^{-1} under nitrogen flow (30 mL min^{-1}). Tensile testing was conducted on a TA-Q series dynamic mechanical analyzer (DMA-Q800, TA Instruments). The ramp force mode with 18 N as upper force limit equipped with a tensile grip holder was used. Samples were carefully loaded into the tensile testing fixture with a preloaded force of 0.001 N and a ramping force of 0.005 N min^{-1} was applied. The test was conducted at room temperature to obtain the stress–strain profile. The Universal Analysis software (TA Instruments) was used to determine stress and strain at break for all samples. Thermomechanical analysis (TMA) was performed using a TA Instruments TMA 2940, a heating rate of 5°C/min in an air atmosphere was used. Samples were crimped-on two cleaved aluminum balls, and suspended in the vertical direction between the probe and stage. Fourier transform infrared spectroscopy (FTIR) was performed using KBr pellets in a Bruker IFS 55 Equinox FTIR spectrophotometer. Electrical conductivity was analyzed using a four-point probe tester, the JANDEL RM2 (Jandel Engineering, USA). Shielding effectiveness (*SE*) of electromagnetic interference (EMI) was conducted using an 8712C RF network analyzer (HEWLETT PACKARD) with a coaxial transmission line fixture developed in house.[23] N_2 adsorption isotherms were measured at 77 K using a Quantachrome NOVA 2200 instrument. The specific surface area (A_{BET}) was calculated from the 0.1–0.3 p/p_0 region of the adsorption isotherm using the Brunauer-Emmett-Teller (BET) method. The pore diameter was calculated by the Barret-Joyner-Halenda (BJH) method from the adsorption isotherm.[2]

Figure 1. Photograph of a Nylon NF mat. [Color figure can be viewed in the online issue, which is available at wileyonlinelibrary.com.]

RESULTS AND DISCUSSION

The developed Nylon NFs are long, homogeneous, beadless, and have a diameter of 280 ± 100 nm (Figure 2). Small samples were cut from the 2 m×1 m×20 μm (length × width × thickness) NF mat (Figure 1). The contact angle of the Nylon NF mat [Figure 3(a)] was measured to be 125°, which is much higher than that of bulk Nylon polymer (70°).[24] The higher surface area and sample roughness provided by the NF structure promote the hydrophobic behavior, even though beneficial, it interferes with the attachment of CNTs onto the NFs in the mat. In order to promote the attachment of CNTs on Nylon NFs, the difference in surface tension (contact angle) should be

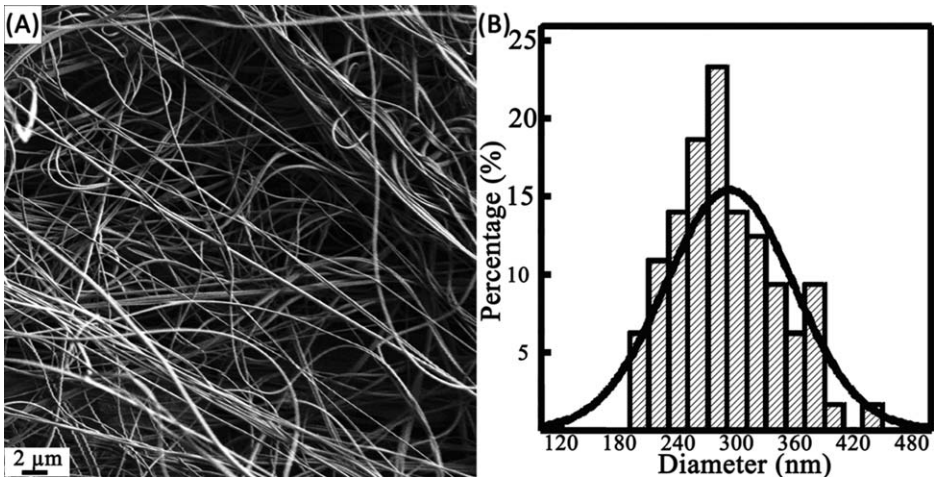

Figure 2. SEM image (a) and diameter distribution histogram (b) of Nylon NFs.

greatly reduced. Surfactants are considered an effective medium and widely used approach to reduce surface tension. Though, surfactant residues on the surface of CNTs could negatively affect the electric conductivity of CNTs. There are some other organic solvents such as dimethylformamide that have proven compatibility with CNTs. However, their toxicity limits the potentials for industrial massive production. TFE is miscible with water and effectively dissolves polyamide. Addition of TFE to the suspension can therefore increase the wetting of Nylon NFs by the aqueous CNT suspension. Once the Nylon NF mat was submerged in a TFE bath, the resultant contact angle was 25° and decayed to zero after three seconds [Figure 3(b,c)]. TFE increases the contact of CNTs with Nylon NFs and hence will increase the interactions of amide groups of Nylon and carboxyl groups of functionalized CNTs (*f*-CNTs). After dipping, the mats were thoroughly washed with water to remove loose CNTs, followed by heat treatment at 140°C. Figure 4(a–c) shows SEM micrographs of the resultant structures, it can be seen that without the TFE, NFs are loosely wrapped by the CNTs. The presence of CNTs within the pores of the NF mat is highly visible. In contrast, the mat dipped in the suspension containing the addition of TFE, resulted in Nylon NFs fully, uniformly, and densely covered with compact CNTs. The pores in the mat are clear and empty [Figure 4(d–f)]. Figure 4(g) shows a photograph of a CNTs covered Nylon NF mat. Table I compares the BET surface area and the pore volume of CNTs, Nylon NF mats, and CNT-Nylon hierarchical NF mats. The Nylon mats have low surface area, no micropores, and negligible volume of mesopores. Whereas the hierarchical NF mats show a remarkable enhancement in surface area and pore volume. Specifically, the surface area of the hierarchical NF mats exhibits eight-fold increase in surface area over that one of the Nylon mats. The hierarchical NF mats exhibit some micropores, which can be attributed to CNTs. Moreover, it is worth noting that compared to both the pure CNTs and Nylon mats, the presence of mesopores in the CNT-Nylon NF mats greatly increases further benefiting applications where large surface area is required.

FT-IR studies were conducted to elucidate understanding of the bonding mechanism occurring in the CNTs coated Nylon NFs. For comparison, carboxylic functionalized CNTs (*f*-CNTs) and pristine Nylon NFs were also investigated. As shown in Figure 5, the intrinsic peak of CNT is at 1631 cm^{-1}, assigned to the C=C stretching vibration mode associated with sidewalls of CNT. After the acid treatment, an additional peak is observed at 1713 cm^{-1}, which is assigned to carboxyl group stretches (–COOH). The broad band at 3450 cm^{-1} is attributed to a –OH stretching in the carboxylic acid group or small quantities of water. Nylon NFs have a peak at 3300 cm^{-1}, assigned to the

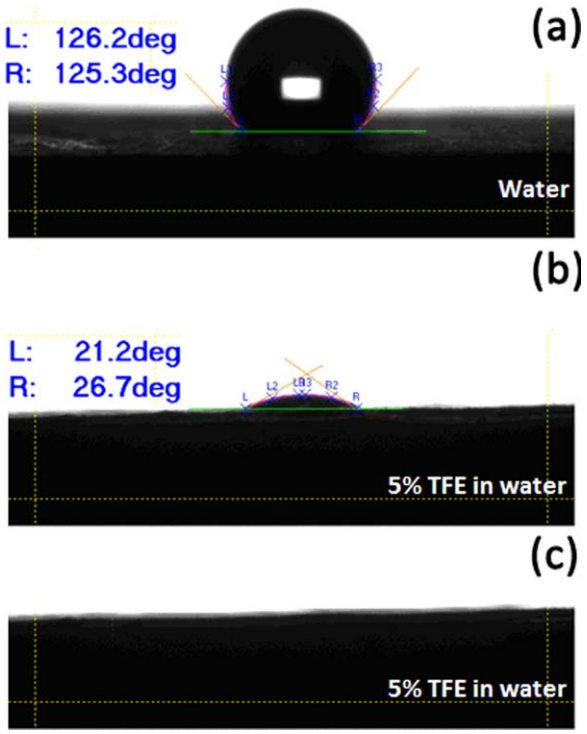

Figure 3. Measurement of contact angles of water droplet (a) and 5% TFE aqueous solution (b, c) on the Nylon NF mat after 2s (a), 3s (c). [Color figure can be viewed in the online issue, which is available at wileyonlinelibrary.com.]

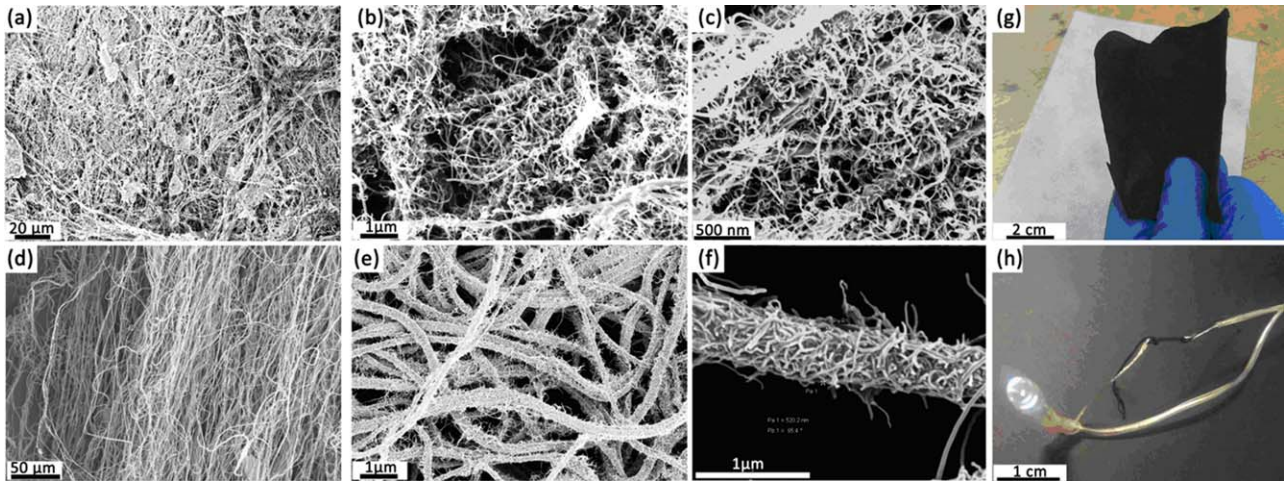

Figure 4. SEM images of Nylon NF mat soaked in CNTs suspension with 5% TFE addition (a–c) and without TFE addition (d–f) for comparison. (g) Photograph of CNT coated Nylon mat and (h) a commercialized light-emitting-diode (LED) lighted using the CNT-Nylon NF mat as the electrical wire. [Color figure can be viewed in the online issue, which is available at wileyonlinelibrary.com.]

Table I. Comparison of BET Surface Area and Pore Volume of CNTs, Nylon NFs and CNTs Coated Nylon NFs with 10 wt % of CNTs

Sample	S_{BET} (m^2 g^{-1})	V_{total} (cm^3 g^{-1})	V_{mic} (cm^3 g^{-1})	V_{mes} (cm^3 g^{-1})
CNTs	60.0	0.139	0.017	0.122
Nylon NFs	1.5	0.005	0	0.005
CNTs/Nylon NFs	12.5	0.269	0.004	0.265

S_{BET}: specific surface area; V_{total}: total pore volume; V_{mic}: micropore volume; V_{mes}, mesopore volume.

amine I bond (NH_2), and two peaks at 1540 and 1641 cm^{-1}, assigned to the amide II bond of Nylon (O=C–NH–C). After the adsorption of CNTs, the peaks corresponding to NH_2 of the Nylon NFs and carboxylic stretches of CNTs disappear. The strong peaks corresponding to O=C–NH–C can still be observed. These observations indicate that the carboxyl groups of the functionalized CNTs (*f*-CNTs) reacted with the amino groups of Nylon NFs generating amide bonds, resulting in the stable attachment of CNTs on the Nylon NFs forming the hierarchical CNT-Nylon NF mat.

The weight percentage of CNTs attached on the NFs was determined through TGA studies. As shown in Figure 6, the amount of CNTs is observed to be 3 wt % for the sample dipped in the

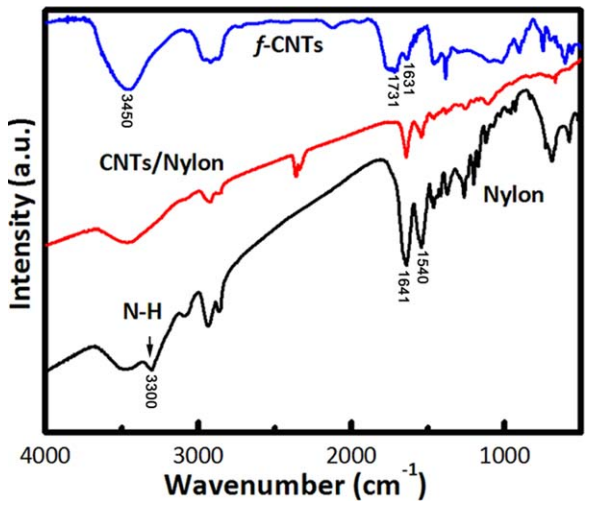

Figure 5. FTIR spectra of functionalized CNTs (*f*-CNTs), Nylon NFs, and CNTs coated Nylon NFs. The peak of N–H bond is labeled with a black arrow. [Color figure can be viewed in the online issue, which is available at wileyonlinelibrary.com.]

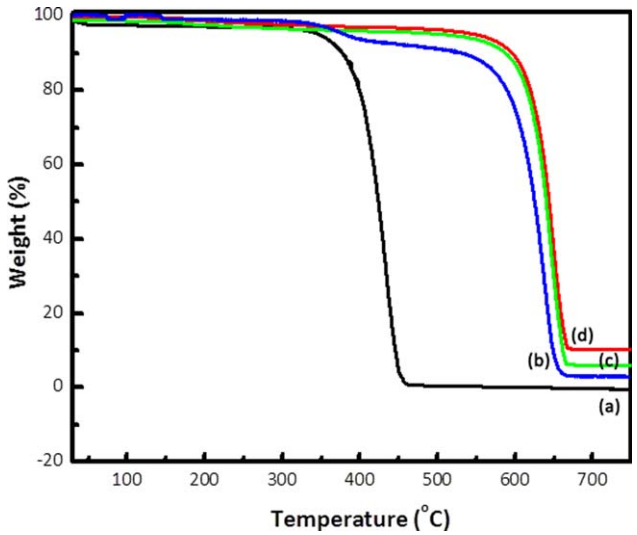

Figure 6. TGA curves of Nylon NFs (a), 3 wt % (b), 6 wt % (c), and 10 wt % (d) CNTs coated Nylon NFs respectively. [Color figure can be viewed in the online issue, which is available at wileyonlinelibrary.com.]

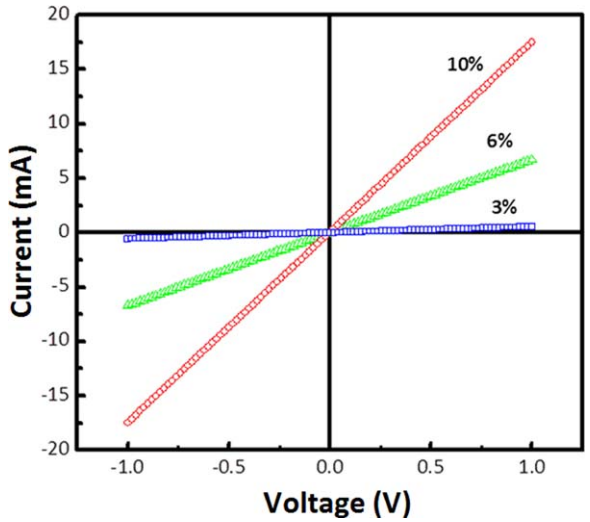

Figure 7. Current-voltage dependence of CNT-Nylon NFs. [Color figure can be viewed in the online issue, which is available at wileyonlinelibrary.com.]

suspension containing 0.5 wt % of CNTs, and the amount increases to 6 and 10 wt %, for the samples dipped in the 1 and 3 wt % CNTs suspension, respectively. Moreover, it can be observed that Nylon NFs start to degrade around 350°C and completely decompose at 460°C, while the sample containing 3 wt % of CNTs have a similar onset degradation temperature, but its quick decomposition temperature increases to 620°C. For the NFs with 6 wt % and 10 wt % of CNTs, the onset temperature increases to 550°C, 200°C higher than that of pure Nylon NFs. These results show that these hierarchical CNT-Nylon NFs mats have a higher thermal stability, due to the uniform and dense adsorption of CNTs onto NFs coupled with the observed covalent bonding (as confirmed by FTIR). The enhanced thermal stability opens up the door to many potential applications.

Figure 7 shows the electrical resistivity of the hierarchical NF mats as a function of CNTs content. It can be seen that the conductivity increases as the CNTs content increases. 3 wt % and 6 wt % of CNTs loaded samples have conductivity of 5×10^{-4} S cm^{-1} and 6×10^{-3} S cm^{-1}, respectively, which are extremely higher than that of Nylon. In particular, the 10 wt % CNT-Nylon NF mat exhibits a conductivity of 0.02 S cm^{-1}. The high electrical conductivity coupled with the retained flexibility of the pure Nylon mat and the enhanced thermal stability allows the usage of the hierarchical NF mats to be used as an effective conductor even if twisted and knotted [Figure 4(h)]. In the absence of TFE, the Nylon mat is coated with randomly distributed CNTs which are also present within the pores of the mat and therefore the percolation threshold of this type of structure becomes similar to that of a conductive film where current travels the path of least resistance. The conductive network is therefore achieved with low amount of CNTs that become in close contact with each other, resembling a 2D percolation process. However, this conductive network can easily be affected by processing and shape changes of the mat, such as twisting, folding, and bending. In the system prepared with TFE, the CNTs only attach on the surface of the NFs preserving the mat structure with empty pores. In this case, the percolation also occurs through tunneling but only along the NFs (1-D percolation process).[25,26] The formation of the CNT network in a 1-D structure has been shown to be more challenging, especially for the aligned CNTs, according to the theoretical prediction by Weber, Kamal, and Lux.[25,26] In order to obtain the percolation, the aligned CNTs on NFs should be in close contact to each other to achieve tunneling along the axes of the NFs. Thus, the percolation threshold is higher than that of conductive thin films.

Electrical and thermo-physical enhancements are promising though as in other systems, the lack of mechanical integrity could hinder potential applications. The results from the characterization of mechanical properties are shown in Figure 8. The pristine Nylon NFs exhibit a tensile strength of 34 MPa. The hierarchical NFs have higher tensile strength and the improvement increases as the CNTs content increases. For instance, 6 wt % CNT-Nylon NFs have a tensile strength of 65 MPa, corresponding to 91% improvement over that of the pure Nylon NFs. In particular, the tensile strength of 10 wt % CNT-Nylon NFs is shown to be 149 MPa, corresponding to 338% enhancement over that of the pure Nylon NFs. Improvements in tensile strength for most of the reported CNTs/polymer composites are coupled with a reduction in strain at break, indicating a decrease in polymer toughness and flexibility.[2,4] For example, Gao *et al.* found that for their SWNT/Nylon composite, the tensile strength increased from 40.9 to 69.1 MPa, whereas the strain at break decreased from 417% to 250% with the incorporation of 1 wt % pristine SWNT in Nylon.[27] In this study, the hierarchical structure system shows an increase in strength coupled with an increase in strain at break. The stress of the hierarchical NFs increases progressively with the presence of CNTs. The strain also increases with the increase of CNT content. Moreover, it is worth mentioning that there is no plateau in the Nylon NFs curve, showing that Nylon NFs break immediately once they are stretched to approximately 160%. On the other side, the developed hierarchical NFs exhibit a plateau, strongly suggesting that the strongly adsorbed and aligned CNTs ultimately carry the load even after polymeric fracture

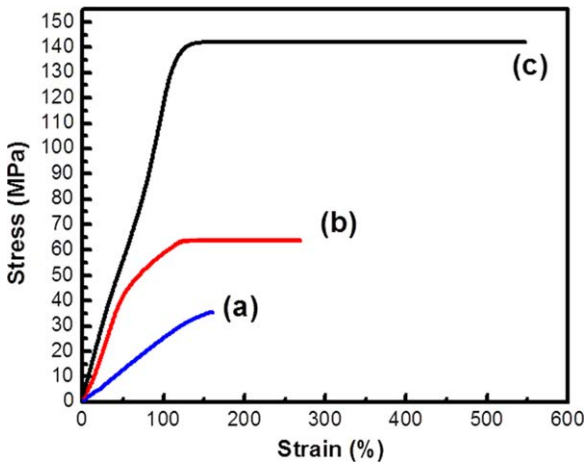

Figure 8. Strength-strain curves of Nylon NFs (a), 6 wt % (b), and 10 wt % (c) CNTs coated Nylon NFs. [Color figure can be viewed in the online issue, which is available at wileyonlinelibrary.com.]

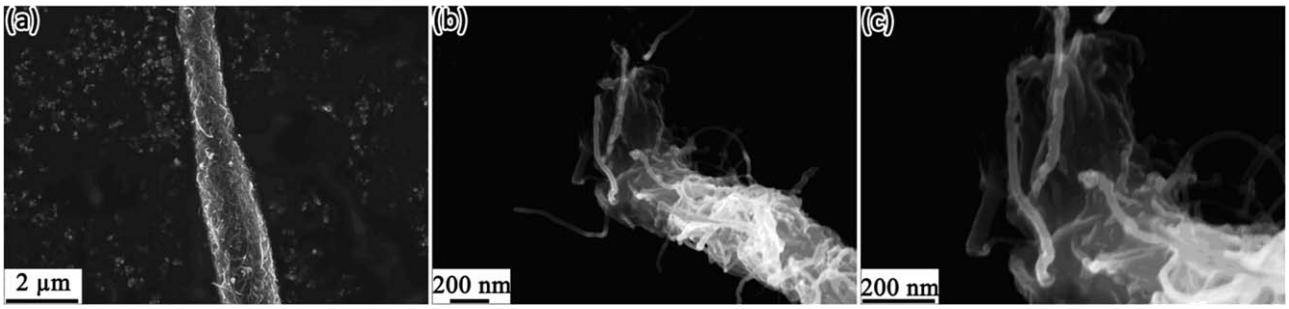

Figure 9. SEM images for elongation (a) and fracture cross-sections (b, c) of CNTs coated Nylon NFs after stretching.

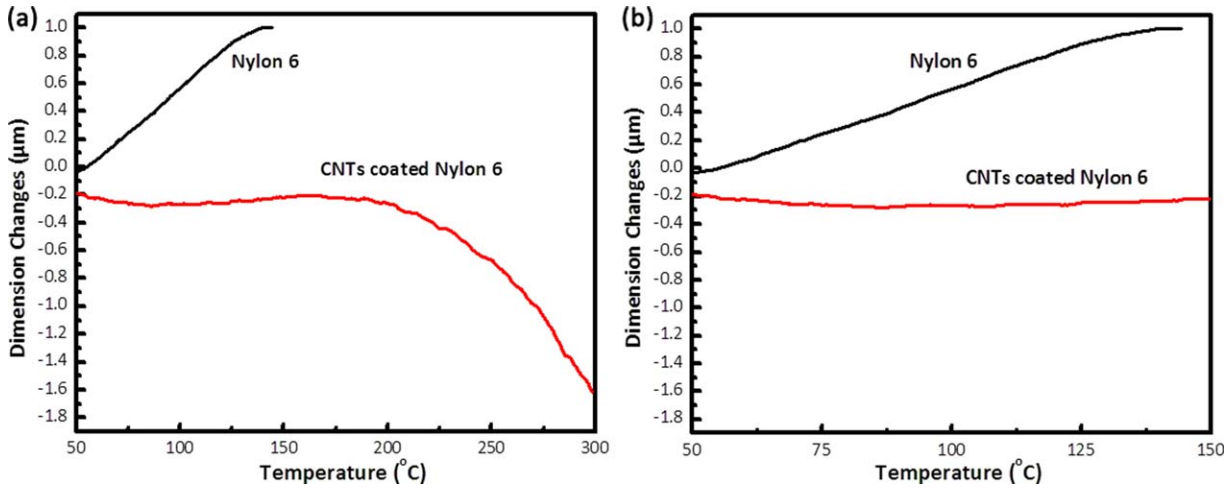

Figure 10. TMA curves of Nylon NFs and 10 wt % CNTs coated Nylon NFs. (b) is a magnified plot of (a) at temperature below 150°C. [Color figure can be viewed in the online issue, which is available at wileyonlinelibrary.com.]

occurred, this can be observed in Figure 8. The presented SEM images (Figure 9) show NF elongation during the tensile testing process, indicating a ductile fracture mechanism for the hierarchical NFs. In Figure 8(b,c), a cross section of the fractured NFs shows a strong adhesion of the CNT to the Nylon NF given the developed covalent bonding as well as Van der Waals forces within the CNTs. These, acted synergistically to improve the overall mechanical integrity. The 10 wt % CNT-Nylon NFs mats were also subjected to TMA analysis. As shown in Figure 10, Nylon NFs has positive thermal expansion coefficient, indicating that Nylon NFs expand with increasing temperature. In contrast, the hierarchical NFs have negligible changes in thermal expansion coefficients at temperatures below 150°C, and exhibit a negative thermal expansion coefficient from 150 to 300°C. The continuous TMA curve well demonstrates that the hierarchical NFs do not break even at 300°C, much higher than the melting temperature of Nylon 6 NFs. Nylon is an insulating polymer with low tensile strength, the conformal coating of CNTs on the NFs in the mat greatly increases both its conductivity and tensile strength. And the hierarchical NF mats have higher conductivity and tensile strength as the CNTs content increases. More importantly, the thermoplastic properties of Nylon are also changed. As a result, CNT-Nylon NFs maintain their shape at temperature below 150°C, and shrink without breaking at higher temperature (below 300°C).

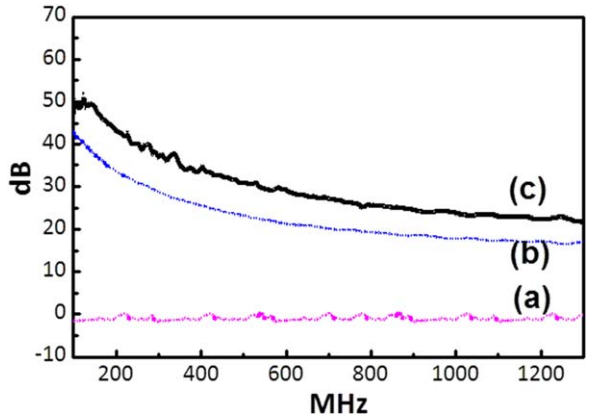

Figure 11. EMI shielding effectiveness as a function of frequency for Nylon mats (a), 6 wt % (b), and 10 wt % (c) CNTs coated Nylon mats. [Color figure can be viewed in the online issue, which is available at wileyonlinelibrary.com.]

The shielding of EMI has been a growing concern given the rapid deployment of commercial and military electronic devices. Materials that could offer EMI shielding besides flexibility, lightweight, corrosion resistance, and suitability for mass production are highly desirable. The EMI shielding effectiveness (*SE*), defined as the logarithmic ratio of incoming power (P_i) to transmitted power (P_t) of an electromagnetic wave (SE (dB) = – 10 log(P_t/P_i)) was measured. Figure 11 shows the plot of EMI

shielding effectiveness (*SE*) vs. varying concentration of adsorbed CNTs. It is observed that the SE of pure Nylon NF mats is zero while that of the hierarchical NF mats increases as the content of CNTs increases. In particular, the hierarchical NF mats with 10 wt % CNTs show a shielding effectiveness (*SE*) of 30 dB.

CONCLUSIONS

This study presents a facile method to mass produce hierarchical CNT-Nylon NF mats. Nylon NF rolls were produced utilizing the forcespinning® (FS) technology. CNTs were covalently bonded to the surface of the Nylon NFs. The hierarchical NFs exhibited polymeric flexibility (given the Nylon substrate) with improvements in surface area, electrical conductivity, and mechanical strength when compared to Nylon NFs. An increase in thermal stability higher than 200°C was observed. In the case of mechanical properties, a dual increase in strength and strain at break was obtained. The EMI shielding effectiveness (*SE*) was found to be 30 dB. The observed properties pose promising applications where flexibility, high strength, electrical conductivity, and thermal stability are needed.

ACKNOWLEDGMENTS

The authors thank Gonglan Yen and Liehui Ge of Rice University for their assistance in materials preparation and characterization. This work was financially supported by National Science Foundation under DMR grant #0934157. Declaration of conflicting interests: Dr. K. L. and the University of Texas-Pan American have research related financial interests with Fiberio Technology Corporation.

REFERENCES

1. Iijima, S. *Nature* **1991**, *354*, 56.
2. Ci, L.; Suhr, J.; Pushparaj, V.; Zhang, X.; Ajayan, P. M. *Nano Lett.* **2008**, *8*, 2762.
3. Li, F.; Scampicchio, M.; Mannino, S. *Electroanalysis* **2011**, *23*, 1773.
4. Kang, M.; Jin, H. J. *Colloid Polym. Sci.* **2007**, *285*, 1163.
5. Lala, N. L.; Thavasi, V.; Ramakrishna, S. *Sensors* **2009**, *9*, 86.
6. Wang, J.; Xu, H.; Yang, D.; Wu, Y. *Fiber Polym.* **2013**, *14*, 571.
7. Luo, C.; Zuo, X.; Wang, L.; Wang, E.; Song, S.; Wang, J.; Wang, J.; Fan, C.; Cao, Y. *Nano Lett.* **2008**, *8*, 4454.
8. Kayser, J. C.; Shambaugh, R. L. *Polym. Eng. Sci.* **1990**, *30*, 1237.
9. Benavides, R. E.; Jana, S. C.; Reneker, D. H. *ACS Macro Lett.* **2012**, *1*, 1032.
10. Lemstra, P. J.; Bastiaansen, C. W. M.; Meijer, H. E. H. *Die Angew. Makromol. Chem.* **1986**, *145*, 343.
11. Sarkar, K.; Gomez, C.; Zambrano, S.; Ramirez, M.; de Hoyos, E.; Vasquez, H.; Lozano, K. Electrospinning to Forcespinning™. *Mater. Today* **2010**, *13*, 12.
12. Xu, F.; Weng, B.; Gilkerson, R.; Materon, L. A.; Lozano, K. *J. Bioact. Compat. Polym.* **2014**, *29*, 646.
13. Xu, F.; Weng, B.; Gilkerson, R.; Materon, L. A.; Lozano, K. *Carbohydr. Polym.* **2015**, *115*, 16.
14. Weng, B.; Xu, F.; Lozano, K. *J. Appl. Polym. Sci.* **2014**, *131*, 40302.
15. Weng, B.; Xu, F.; Lozano, K. *Carbon* **2014**, *75*, 217.
16. Weng, B.; Xu, F.; Garza, G.; Alcoutlabi, M.; Salinas, A.; Lozano, K. *Polym. Eng. Sci.* **2014**, *55*, 81.
17. McEachin, Z.; Lozano, K. *J. Appl. Polym. Sci.* **2012**, *126*, 473.
18. Altecor, A.; Mao, Y. B.; Lozano, K. *Funct. Mater. Lett.* **2012**, *5*, 1250020.
19. Ouyang, Z.; Li, J.; Wang, J.; Li, Q.; Ni, T.; Zhang, X.; Wang, H.; Li, Q.; Su, Z.; Wei, G. *J. Mater. Chem. B* **2013**, *1*, 2415.
20. Su, Z.; Li, Q.; Ni, T.; Wei, G. *Carbon* **2012**, *50*, 5605.
21. Su, Z.; Ding, J.; Wei, G. *RSC Adv.* **2014**, *4*, 52598.
22. Lozano, K.; Files, B.; Rodriguez-Macias, F.; Barrera, E. V. *TMS Publications* **1999**, *3*, 333.
23. Vasquez, H.; Espinoza, L.; Lozano, K.; Foltz, H.; Yang, S. IEEE Transactions on Electromagnetic Compatibility; Practical Papers, Articles and Applications Notes, volume 220, 62 pp., **2009**.
24. Mittal, K. L. Polymer Surface Modification: Relevance to Adhesion. VSP: Utrecht: The Netherlands, **2004**; Vol. 3, p 129.
25. Lux, F. *J. Mater. Sci.* **1993**, *28*, 285.
26. Weber, M.; Kamal, M. R. *Polym. Compos.* **1997**, *18*, 711.
27. Gao, J.; Zhao, B.; Itkis, M. E.; Bekyarova, E.; Hu, H.; Kranak, V.; Yu, A.; Haddon, R. C. *J. Am. Chem. Soc.* **2006**, *128*, 7492.